Synthesis, characterization and crystal structure of oxobis(*p*-thiocresolato)terpyridinerhenium(V), a new cationic, six-coordinate thiolato complex of rhenium

Lihsueh (Sherry) Chang, Jochen Rall†, Francesco Tisato†, Edward Deutsch*,†
Biomedical Chemistry Research Center, Department of Chemistry, University of Cincinnati, Cincinnati, OH 45221-0172 (USA)
and Mary Jane Heeg*
Department of Chemistry, Wayne State University, Detroit, MI 48202-3929 (USA)

(Received September 14, 1992)

Abstract

The new six-coordinate rhenium(V) complex, oxobis(*p*-thiocresolato)terpyridinerhenium(V), was synthesized from $[ReO_2(py)_4]CF_3SO_3$ and characterized by elemental analysis, thin-layer chromatography, FAB mass spectroscopy, IR and ^1H NMR of the perrhenate salt, as well as by a single crystal X-ray structure determination of the hexafluorophosphate salt. This characterization establishes the structure of the complex in both solid state and solution to be the symmetrical *mer(N,N,N),trans(S,S)* species in which the central N atom of the terpyridine ligand is situated *trans* to the Re=O linkage. The X-ray and NMR studies demonstrate that the solution and solid state structures are identical.

Introduction

So far, only a few rhenium(V) complexes with monodentate thiolato ligands have been described in the literature [1–5], all of which have the coordination number five. This report presents the synthesis of a novel six-coordinate rhenium(V)–thiolato complex and is also the first rhenium–terpyridine complex to be structurally characterized; $[ReO(SC_6H_4Me\text{-}p)_2(terpy)]^+$ is diagrammed below.

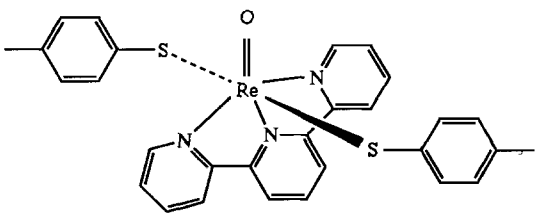

This work is part of our continuing investigations into thiolato complexes of rhenium [6, 7] and technetium [8–13] and polypyridyl complexes of technetium [14, 15]. Our desire to prepare mixed ligand polypyridyl–thiolato complexes sprang from the expectation that the flexibility of R group manipulations in SR^- ligands could be combined with the advantages of chelated coligands to generate a family of potentially useful radiopharmaceuticals. In theory, at least, expression of the chelate effect produces higher formation constants relative to those for related mono-ligands, reduced susceptibility to metathesis in the product and fewer side products in the formation reaction. These are desirable characteristics for potential radiopharmaceutical complexes for which a simple, clean preparative reaction and product stability are important [16].

Acronyms and abbreviations

The following acronyms and abbreviations are used in this article: bpy = 2,2′-bipyridine; COSY = two-dimensional homonuclear shift correlation; dip = diphosphine; FAB-MS = fast atom bombardment mass spectrometry; py = pyridine; terpy = 2,2′:6′,2″-terpyridine; TLC = thin layer chromatography.

*Authors to whom correspondence should be addressed.
†Current addresses: Dr Jochen Rall, Kantstrasse 11, W-7014 Kornwestheim, Germany; Dr. Francesco Tisato, Consiglio Nazionale delle Ricerche, Instituto di Chimica e Technologia dei Radioelementi, Corso Stati Uniti 4, 35020 Padua, Italy; Dr Edward A. Deutsch, Mallinckrodt Medical, Inc., 675 McDonnell Blvd., P.O. Box 5840, St. Louis, MO 63134, USA.

0020-1693/93/$6.00

Experimental

Reagents

Ammonium perrhenate (99+%), *p*-thiocresol and lithium trifluoromethanesulfonate (97%) were purchased from Aldrich. 2,2′:6′,6″-Terpyridine was obtained from G. F. Smith Chemicals. Pyridine and all solvents were supplied by Fisher and used without further purification.

Measurements

Thin layer chromatographic plastic sheets (silica gel 60 F_{254}, layer thickness 0.2 mm) from E. Merck were used. The mobile phase was HPLC-grade acetonitrile/0.1 M CF_3SO_3Li. The elemental analysis was performed by Galbraith Laboratories, Knoxville, TN. IR spectra were recorded on a Perkin-Elmer 1600 Series FT-IR spectrometer in KBr pellets. FAB-MS were recorded on a VG-30-250 Masslab instrument in positive ion mode for cations and in negative ion mode for anions. The FAB-MS experimental conditions were: flux, 3×10^{-5} mbar; voltage, 7 kV; ion current, 1 mA; ion type, xenon cations; temperature, ambient; matrix, *m*-nitrobenzylalcohol. ^1H NMR studies were conducted on a Bruker AC-250 spectrometer. X-ray diffraction data were collected on a Nicolet $P2_1$ automated diffractometer using Cu Kα radiation and a graphite monochromator at ambient temperature. Experimental details for the crystallographic experiment are given in Table 1. Table 2 contains the fractional atomic coordinates.

Synthesis of [$ReOCl_2(OEt)(PPh_3)_2$]

Dichlorooxoethoxobis(triphenylphosphine)rhenium(V) was prepared by a slight variation of a reported method [17]. 1 g of NH_4ReO_4 (3.73 mmol) was suspended in 2.5 ml 37% HCl (30 mmol) and added to a solution of 5 g PPh_3 (19 mmol) in 30 ml ethanol. After 10 min boiling under reflux, the product was removed by filtration, washed with ethanol and ethyl ether and dried. A grey–green powder, soluble in benzene, chloroform and dichloromethane, is obtained

TABLE 1. Crystallographic data for [$ReO(SC_6H_4Me$-*p*$)_2$(terpy)]PF_6

Formula	$Re_1S_2P_1F_6O_1N_3C_{29}H_{25}$
Formula weight (amu)	826.83
Space group	*C*2/*c* (No. 15)
a (Å)	8.4505(8)
b (Å)	27.059(9)
c (Å)	26.285(4)
β (°)	92.92(1)
V (Å^3)	6002(2)
Z	8
T (°C)	20
λ (Å)	1.54178
ρ(calc.) (g cm^{-3})	1.830
μ (cm^{-1})	100.25
Transmission coefficients	0.283–0.133
R [a]	0.038
R_w [a]	0.042

[a] $R=(\Sigma|\Delta F|)/\Sigma|F_o|$; $R_w=[(\Sigma w|\Delta F|^2)/\Sigma wF_o^2]^{1/2}$.

TABLE 2. Fractional atomic coordinates for [$ReO(SC_6H_4Me$-*p*$)_2$(terpy)]PF_6

Atom	*x*	*y*	*z*
Re1	0.29812(4)	0.40626(1)	0.01682(1)
S1	0.0511(3)	0.44149(7)	0.03719(8)
S2	0.4859(3)	0.35490(7)	−0.02224(8)
O1	0.4215(7)	0.4431(2)	0.0514(2)
N1	0.2762(7)	0.3454(2)	0.0646(2)
N2	0.1332(7)	0.3547(2)	−0.0219(2)
N3	0.2384(8)	0.4375(2)	−0.0548(2)
C1	0.356(1)	0.3412(3)	0.1100(3)
C2	0.346(1)	0.3023(3)	0.1414(3)
C3	0.247(1)	0.2645(3)	0.1284(3)
C4	0.162(1)	0.2664(3)	0.0827(3)
C5	0.1768(9)	0.3075(3)	0.0514(3)
C6	0.0914(9)	0.3137(3)	0.0015(3)
C7	−0.025(1)	0.2823(3)	−0.0207(3)
C8	−0.092(1)	0.2954(3)	−0.0676(3)
C9	−0.044(1)	0.3378(3)	−0.0921(3)
C10	0.0710(9)	0.3671(3)	−0.0687(3)
C11	0.1363(9)	0.4124(3)	−0.0882(3)
C12	0.104(1)	0.4309(3)	−0.1366(3)
C13	0.172(1)	0.4733(3)	−0.1518(3)
C14	0.275(1)	0.4993(3)	−0.1180(3)
C15	0.304(1)	0.4796(3)	−0.0698(3)
C16	−0.027(1)	0.4024(3)	0.0846(3)
C17	−0.157(1)	0.3728(3)	0.0717(3)
C18	−0.209(1)	0.3395(4)	0.1067(4)
C19	−0.139(1)	0.3352(4)	0.1549(4)
C20	−0.190(2)	0.2952(5)	0.1907(5)
C21	−0.016(1)	0.3672(4)	0.1679(4)
C22	0.042(1)	0.4002(3)	0.1333(3)
C23	0.554(1)	0.3854(3)	−0.0764(3)
C24	0.515(1)	0.3677(3)	−0.1251(4)
C25	0.575(1)	0.3907(4)	−0.1665(4)
C26	0.669(1)	0.4322(4)	−0.1618(4)
C27	0.732(1)	0.4578(4)	−0.2087(4)
C28	0.709(1)	0.4499(3)	−0.1131(4)
C29	0.652(1)	0.4271(3)	−0.0715(4)
P1	0.50000	0.1820(2)	0.25000
F1	0.50000	0.1254(4)	0.25000
F2	0.50000	0.2376(4)	0.25000
F3	0.376(2)	0.1810(4)	0.2907(4)
F4	0.364(2)	0.1796(4)	0.2066(4)
P2	0.50000	0.4124(3)	0.25000
P2′	0.448(2)	0.4134(7)	0.2613(6)
F5	0.50000	0.3573(6)	0.25000
F6	0.325(2)	0.4129(4)	0.2294(5)
F7	0.497(3)	0.4316(9)	0.3040(9)
F8	0.433(3)	0.3895(8)	0.3039(9)
F9	0.441(2)	0.4613(5)	0.2775(6)

in almost quantitative yield (*c.* 3.1 g). $M = 842.75$ g/mol.

Synthesis of $[ReO_2(py)_4]Cl \cdot 2H_2O$

Dioxotetrapyridinerhenium(V) chloride dihydrate was prepared by adding dropwise 5 ml pyridine (62 mmol) to a suspension of 1 g $[ReOCl_2(OEt)(PPh_3)_2]$ (1.19 mmol) in 25 ml ethanol. The reaction mixture was boiled under reflux for 2 h. The resulting brown solution was filtered, if necessary, and concentrated to 10 ml on a rotary evaporator. The yellow–orange product was precipitated by dropwise addition of ethyl ether, removed by filtration, washed with ether and dried. Yield 95%, *c.* 0.7 g. $M = 606.08$ g/mol.

Synthesis of $[ReO_2(py)_4]CF_3SO_3 \cdot 2H_2O$

Dioxotetrapyridinerhenium(V) trifluoromethanesulfonate dihydrate was prepared by dissolving 0.7 g $[ReO_2(py)_4]Cl \cdot 2H_2O$ (1.15 mmol) in 60 ml of an ethanol/water mixture (50/50), containing about 2% pyridine to avoid decomposition. A green, insoluble impurity, which sometimes formed, was removed by filtration. Then 1.5 g CF_3SO_3Li (9.6 mmol), dissolved in water, was added. The solution was concentrated on a rotary evaporator and the product was removed by filtration, washed with cold ethanol/ether and ether, and dried *in vacuo*. Yield 50%, *c.* 0.4 g. $M = 719.7$ g/mol.

Synthesis of $[ReO(SC_6H_4Me\text{-}p)_2(terpy)]ReO_4$

Oxobis(*p*-thiocresolato)terpyridinerhenium(V) perrhenate was prepared by dissolving 720 mg $[ReO_2(py)_4]CF_3SO_3 \cdot 2H_2O$ (1.0 mmol) in 40 ml ethanol. Then 250 mg 2,2′:6′,6″-terpyridine (1.1 mmol) and 250 mg *p*-thiocresol (2.0 mmol) were added. The reaction mixture was boiled under reflux for 18 h, after which a dark brown solution was obtained. This solution was diluted with *c.* 20 ml water and the solvent then partially evaporated under vacuum. The black crystals which formed were washed with water and recrystallized from an acetone/water mixture. Yield up to 44%, *c.* 400 mg. $M = 923.07$ g/mol. *Anal.* Calc. for $[ReO(SC_6H_4Me\text{-}p)_2(terpy)]ReO_4$: C, 37.4; H, 2.7; N, 4.5; S, 6.9. Found: C, 38.8; H, 2.7; N, 4.7; S, 7.5%. The high percentages found for the carbon and sulfur analyses indicate that the anion is partially $CF_3SO_3^-$. The product is soluble in acetone, acetonitrile, methanol, ethanol, dichloromethane and chloroform, yielding solutions that are yellow to brown in color; it is insoluble in water, ether and toluene. It can be recrystallized from acetone/water, acetone/toluene, dichloromethane/toluene, or ethanol to form black needles or plates. It is quite stable, but NMR shows some decomposition after one month in acetone. Note: the anion is mostly ReO_4^- under these conditions, but some $CF_3SO_3^-$ can be present. Precipitation with HPF_6 does not replace all ReO_4^-, and therefore precipitation with NH_4ReO_4 is recommended.

Results and discussion

Synthesis and reactivity

The six-coordinate oxobis(*p*-thiocresolato)terpyridinerhenium(V) cation was first obtained in an attempt to synthesize rhenium(III) complexes. Refluxing $[ReO_2(py)_4]CF_3SO_3$ in the presence of *p*-thiocresol and terpyridine for 17 h in an ethanol/water mixture yields a black precipitate and an almost black solution. TLC, FAB-MS and NMR characterization show that the precipitate is the rhenium(V) complex $[ReO(SC_6H_4Me\text{-}p)_2(terpy)]^+$.

In addition to the product, the reaction mixture contains several other rhenium complexes. TLC is a good indicator for these complexes and may be used to monitor the reaction and check the purity of the isolated rhenium(V) product. The different complexes can be separated by column chromatography, using silica gel as the stationary phase and acetonitrile, containing 0.1 M CF_3SO_3Li, as the mobile phase. This technique allows characterization of some of the byproduct complexes by UV–Vis spectroscopy, IR, ^1H NMR or FAB-MS. One of the byproducts which often contaminates the product and cannot be removed by recrystallization is characterized as $[ReO(SC_6H_4Me\text{-}p)_4]^-$. This known complex [3] is formed early in the reaction, in reactions conducted at lower temperatures and in reactions conducted with excess *p*-thiocresolate. It might be a key intermediate, the formation of which is kinetically favored, since its generation requires only a simple ligand exchange reaction. Moreover, at least three other compounds are formed; these are probably the three $[Re^{III}(terpy)_2X]^{2+}$ complexes with $X = OH^-$, $C_2H_5O^-$ and $^-SC_6H_4Me\text{-}p$. The complex with $X = OH^-$ has been completely characterized and will be described in a future publication [18].

The generation of rhenium(III) compounds establishes that some reduction of the rhenium(V) starting material occurs during the reaction. Elemental analysis of the title rhenium(V) product, an intense peak at 903 cm^{-1} in the IR spectrum, and FAB-MS analyses in the negative ion mode, show that ReO_4^- is always present, even after precipitation with CF_3SO_3Li or KPF_6. This implies that disproportionation of rhenium(V) to rhenium(III) and rhenium(VII) takes place during the synthetic reaction. This disproportionation appears to be favored at higher temperatures and longer reaction times. The rhenium(III) complexes and the very stable perrhenate ion might be thermodynamically more favorable than the rhenium(V) product.

The theoretical yield of $[ReO(SC_6H_4Me\text{-}p)_2(terpy)]ReO_4$ should be 33% if perrhenate is the anion associated with the rhenium(V) product. The observation of somewhat higher yields and anion analyses by FAB-MS lead to the conclusion that other anions such as $CF_3SO_3^-$, PF_6^- or excess $^-SC_6H_4Me\text{-}p$ do co-crystallize with the cationic title complex.

Other reaction conditions were investigated to try to improve the yield. Reaction in acetone produces less rhenium(III), but some ReO_4^- can also be detected. Using the monooxo rhenium(V) complexes $[ReO(X)_2(OEt)(PPh_3)_2]$ (X = Cl, Br, I) as starting materials leads to the desired product in only 30 min, significantly less time than is required when $[ReO_2(py)_4]CF_3SO_3$ is the starting material (17 h). In addition, the yield is improved (65%) and the disproportionation is mostly avoided. However, the separation and purification of the product is more difficult as a result of the different composition of the byproducts. $[ReO(Br)_2(OEt)(PPh_3)_2]$ seems to be the best starting material of this group since the chloro, and especially the iodo analogs, yield more complex byproduct mixtures.

Characterization

$[ReO(SC_6H_4Me\text{-}p)_2(terpy)]ReO_4$ is characterized by elemental analysis, TLC, FAB-MS, IR spectroscopy, ^1H NMR spectroscopy and a single crystal analysis of the PF_6^- salt. The elemental analysis is given in 'Experimental' and indicates that a mixture of anions is associated with the rhenium cation. The composition of the complex cation is more reliably made by positive ion mode FAB-MS, which is presented in Table 3 and clearly shows the parent ion M^+ and $M^+ - (SC_6H_4Me)$ with the expected isotopic ratios for $^{185/187}Re$. The TLC retention factors for $[ReO(SC_6H_4Me\text{-}p)_2(terpy)]^+$ and several other byproducts of the synthetic reaction are listed in Table 4.

IR spectroscopy

The IR spectrum of $[ReO(SC_6H_4Me\text{-}p)_2(terpy)]ReO_4$ was obtained in a KBr pellet and is summarized in Table 5. The five most intense peaks are in the region 750–1500 cm^{-1} and are assigned by comparison to literature data and to the spectrum of the uncoordinated (free) terpyridine compound. The spectrum is dominated by an intense peak at 903 cm^{-1} which is attributed to the perrhenate anion. All the spectra of $KReO_4$, NH_4ReO_4 and $Ba(ReO_4)_2 \cdot 2H_2O$ contain an intense, broad peak in the range 890–940 cm^{-1} [19]. The absorption at 955 cm^{-1} results from the terminal rhenium–oxo stretch $\nu(Re{=}O)$. For monooxo–rhenium(V) complexes, it occurs typically between 912 and 995 cm^{-1} [20]. Specifically in $[ReO(SR)_4]^-$ complexes, this $\nu(Re{=}O)$ vibration is reported to be in the range 949–960 cm^{-1} [2, 3]. The other major peaks at 772, 1384 and 1450 cm^{-1} are assigned to vibrations of the coordinated terpyridine ligand. In the spectrum of the free terpyridine, they occur at 762, 1384 and 1455 cm^{-1}.

TABLE 3. FAB-MS data for $[ReO(SC_6H_4Me\text{-}p)_2(terpy)]ReO_4$

m/z	Relative intensity (%)	Assignment
558/560	29/52 = 0.56[a]	$[ReO(SC_6H_4Me\text{-}p)(terpy)]^+$
681/683	20/38 = 0.53[a]	$[ReO(SC_6H_4Me\text{-}p)_2(terpy)]^+$

[a]Theoretical isotopic ratio for $^{185}Re/^{187}Re$ is 37/63 = 0.59.

TABLE 4. TLC retention factors for $[ReO(SC_6H_4Me\text{-}p)_2(terpy)]ReO_4$ and reaction byproducts[a]

Complex	R_f	Color
$[Re(terpy)_2OH]^{2+}$	0.10[b]	red
$[Re(terpy)_2(OEt)]^{2+}$ [c]	0.39	red
$[Re(SC_6H_4Me\text{-}p)(terpy)_2]^{2+}$ [c]	0.60	orange
$[ReO(SC_6H_4Me\text{-}p)_2(terpy)]^+$	0.80	yellow
$[ReO(SC_6H_4Me\text{-}p)_4]^-$	0.99	brown

[a]The conditions are given in 'Experimental'. Note that the R_f values are very dependent on the concentration of CF_3SO_3Li. [b]Ref. 18. [c]Tentative assignment; not characterized.

TABLE 5. IR spectroscopic data for $[ReO(SC_6H_4Me\text{-}p)_2(terpy)]ReO_4$ [a]

Wavenumber (cm^{-1})	Assignment
504	
772	terpyridine
818	
903	ReO_4^-
955	Re=O
1384	terpyridine
1450	terpyridine
1480	
1604	

[a]Major peaks from 500 to 1800 cm^{-1} are noted, in KBr pellet.

^1H NMR spectroscopy

Proton nuclear magnetic resonance has played a major role in the determination of the solution structure of the complex $[ReO(SC_6H_4Me\text{-}p)_2(terpy)]ReO_4$. The COSY experiment is a two-dimensional homonuclear shift correlation technique that maps out all homonuclear couplings in an NMR spectrum. Both axes correspond to proton chemical shift scales. The normal proton spectrum appears along the diagonal while all off-diagonal spots correspond to ^1H–^1H homonuclear

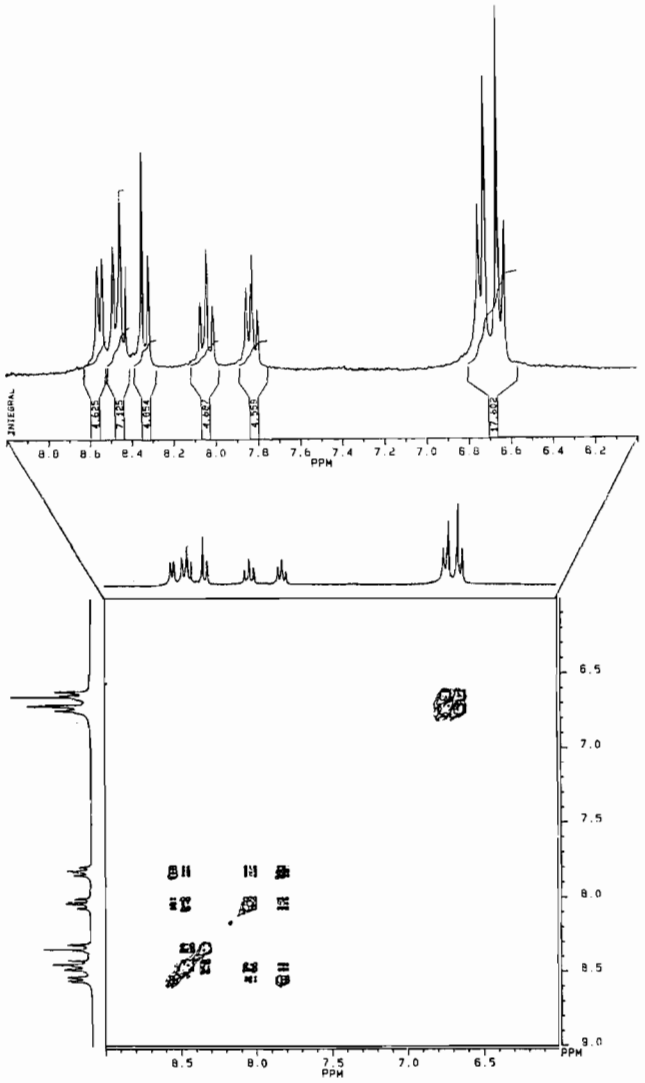

Fig. 1. 250 MHz COSY ^{1}H NMR spectrum of [ReO(SC_6H_4Me-*p*)$_2$(terpy)]ReO_4 in acetone-d^6 over the aromatic region (6.0–9.0 ppm).

couplings. The spectra of the aromatic region of the title complex are presented in Figs. 1 and 2, and in tabular form in Tables 6–8. Labeling of the protons in both spectra is according to the diagrams below.

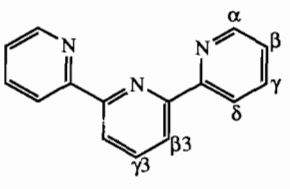

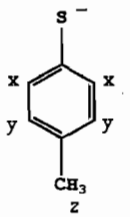

Terpyridine ^{1}H NMR spectrum

At high resolution, the 250 MHz spectrum of terpyridine exhibits six proton signals of varying multiplicities (Table 6). Thus, of the eleven protons in the

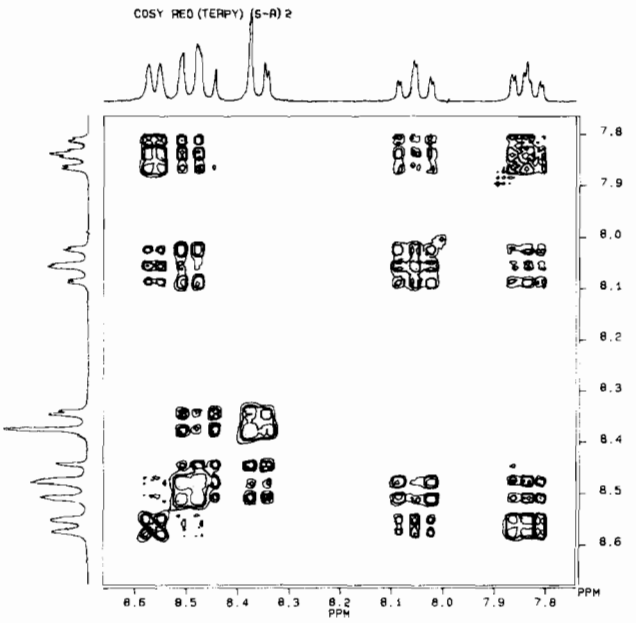

Fig. 2. 250 MHz COSY ^{1}H NMR spectrum of [ReO(SC_6H_4Me-*p*)$_2$(terpy)]ReO_4 in acetone-d^6 including the terpyridine protons only.

molecule there are five pairs of magnetically equivalent ones, as expected from symmetry considerations. The triplet of the γ_3 signal is easily recognized since it is the only one for which the integration corresponds to one proton. The β_3 signal is the only true doublet and is coupled with the γ_3 signal. The assignment of the four proton signals of the lateral pyridine rings is based on the following observations and conclusions. (i) The α signal is shifted most downfield, because it is closest to the electronegative nitrogen atom. It is not only a doublet, but a doublet of a doublet due to the long range coupling with the γ proton. Coupling over four bonds is generally observed in the terpy system. (ii) H_β exhibits a complex ddd-multiplet signal, because it is coupled to all other protons in the ring with different coupling constants. H_β is the most upfield signal. (iii) The γ signal shows similar coupling, but since H_β and H_δ are more similar than H_α and H_γ, it appears more simply as a doublet of a triplet. (iv) The δ signal overlaps partly with the α signal, but a close examination of the COSY spectrum shows that these two signals are not coupled with each other. The chemical shifts listed in Table 6 were reproducible to within ± 0.04 ppm.

[ReO(SC_6H_4Me-p)$_2$(terpy)]ReO_4 ^{1}H NMR spectrum

The spectrum of the rhenium complex is illustrated in Figs. 1 and 2 and tabulated in Table 7. Three well-defined groups of signals are easily distinguishable. (i) There is a sharp singlet occurring at 2.18 ppm with a relative integration corresponding to six protons; this is assigned to the methyl group of the *p*-thiocresolato

TABLE 6. ^{1}H NMR data for terpyridine in acetone-d^6

Proton	δ (ppm)	Multiplicity[a]	Coupling	Relative integration
H_α	8.71	dd	$^3J(H_\alpha H_\beta) = 4.8$ Hz $^4J(H_\alpha H_\gamma) = 1.6$ Hz	2H
H_δ	8.69	dd	$^3J(H_\delta H_\gamma) = 7.8$ Hz $^4J(H_\delta H_\beta) = 1.1$ Hz	2H
$H_{\beta 3}$	8.54	d	$^3J(H_{\beta 3} H_{\gamma 3}) = 7.9$ Hz	2H
$H_{\gamma 3}$	8.08	t	$^3J(H_{\gamma 3} H_{\beta 3}) = 7.9$ Hz	1H
H_γ	7.98	dt	$^3J(H_\gamma H_\delta = H_\gamma H_\beta) = 7.8$ Hz $^4J(H_\gamma H_\alpha) = 1.6$ Hz	2H
H_β	7.46	ddd(m)	$^3J(H_\beta H_\gamma) = 7.8$ Hz $^3J(H_\beta H_\alpha) = 4.8$ Hz $^4J(H_\beta H_\delta) = 1.1$ Hz	2H

[a]s = singlet; d = doublet; t = triplet; m = multiplet; dd = doublet of doublet; dt = doublet of triplet; ddd = doublet of doublet of doublet.

TABLE 7. ^{1}H NMR data for $[ReO(SC_6H_4Me\text{-}p)_2(terpy)]ReO_4$ in acetone-d^6

Proton	δ (ppm)	Multiplicity[a]	Coupling	Relative integration
H_α	8.56	d	$^3J(H_\alpha H_\beta) = 5.8$ Hz	2H
H_δ	8.49	d	$^3J(H_\delta H_\gamma) = 7.8$ Hz	2H
$H_{\gamma 3}$	8.48	t	$^3J(H_{\gamma 3} H_{\beta 3}) = 7.0$ Hz	2H
$H_{\beta 3}$	8.37	d	$^3J(H_{\beta 3} H_{\gamma 3}) = 7.0$ Hz	1H
H_γ	8.06	dt	$^3J(H_\gamma H_\delta = H_\gamma H_\beta) = 7.8$ Hz $^4J(H_\gamma H_\alpha) = 1.4$ Hz	2H
H_β	7.85	ddd(m)	$^3J(H_\beta H_\gamma) = 7.8$ Hz $^3J(H_\beta H_\alpha) = 5.8$ Hz $^4J(H_\beta H_\delta) = 1.3$ Hz	2H
H_x	6.75	d	$^3J(H_x H_y) = 8.0$ Hz	4H
H_y	6.67	d	$^3J(H_y H_x) = 8.0$ Hz	4H
H_z	2.18	s		6H

[a]s = singlet; d = doublet; t = triplet; m = multiplet; dd = doublet of doublet; dt = doublet of triplet; ddd = doublet of doublet of doublet.

TABLE 8. Comparison of the chemical shifts of proton signals in $[ReO(SC_6H_4Me\text{-}p)_2(terpy)]ReO_4$ and in non-coordinated terpyridine and *p*-thiocresol in acetone-d^6

Proton	$\delta_{complex}$	$\delta_{free\ ligand}$	$\Delta\delta$
H_α	8.56	8.71	−0.15
H_β	7.85	7.46	+0.39
H_γ	8.06	7.98	+0.08
H_δ	8.49	8.69	−0.20
$H_{\beta 3}$	8.37	8.54	−0.17
$H_{\gamma 3}$	8.48	8.08	+0.40
H_x	6.75	7.20	−0.45
H_y	6.67	7.07	−0.40
H_z	2.18	2.26	−0.08

ligands. (ii) Two coupled doublets (of the AB type pattern), having relative integration heights corresponding to eight protons, are observed between 6.6 and 6.8 ppm; these arise from the two pairs of aromatic protons in the *p*-thiocresolato ligands. Their coupling with each other, but with none of the terpy protons, can be seen in the COSY spectrum of Fig. 1 without difficulty. (iii) Assignment of the terpyridine proton signals in the region from 7.8 to 8.6 ppm is made by means of similar considerations used to interpret the spectrum of the free ligand (*vide supra*).

The relative simplicity of its ^{1}H NMR spectrum establishes the high symmetry of the rhenium complex in solution. Both *p*-thiocresolato ligands are equivalent. The symmetry plane of the central ring of terpyridine is conserved when the ligand is coordinated to the metal; otherwise eleven proton signals would be observed instead of six. These facts can only be explained within a *mer*(*N*,*N*,*N*),*trans*(*S*,*S*) configuration in which the central nitrogen atom of the terpy ligand is situated *trans* to the Re=O linkage. A comparison of proton chemical shifts in the complex and in the free ligand is given in Table 8.

Crystallography of [ReO(SC_6H_4Me-p)$_2$(terpy)]PF_6

The structural analysis confirms the *mer*(*N*,*N*,*N*),-*trans*(*S*,*S*) configuration of the cation [ReO(SC_6H_4Me-*p*)$_2$(terpy)]$^+$ in the solid state, in full agreement with that deduced from the ^{1}H NMR solution spectrum. Figure 3 illustrates the geometry of the cation and its assigned atom labeling. Selected bond lengths and angles are given in Table 9. All atoms in the cation occupy general positions in the unit cell. Two half PF_6^- anions are present on special (two-fold) positions, one of which is disordered.

Generally, rhenium(V)–monooxothiolato complexes are square pyramidal and five-coordinate. Most technetium(V) monooxo complexes also adopt this coordination, but for rhenium(V), a distorted octahedral configuration is more common and five-coordinate species often readily increase their coordination number to six by weakly binding a solvent molecule *trans* to the Re=O linkage [21]. However, in rhenium(V)–monooxo–thiolato complexes, the coordination number is rarely increased to six [22]. In [ReO(SC_6H_4Me-*p*)$_2$(terpy)]$^+$ the neutral terpy ligand coordinates more readily opposite the strong σ-and π-donor oxo ligand, than do anionic ligands, in part due to the π-acceptor ability of the terpy ligand and the additional stability engendered by the chelate effect. The central nitrogen atom of the terpy ligand has a longer Re–N length than do the distal nitrogen atoms, showing that the structural *trans* effect [23] of the *trans* oxo group is strongly transmitted to the central nitrogen atom. In *all* other terpy–metal complexes, the central M–N bond length is characteristically shorter than those terminal [24].

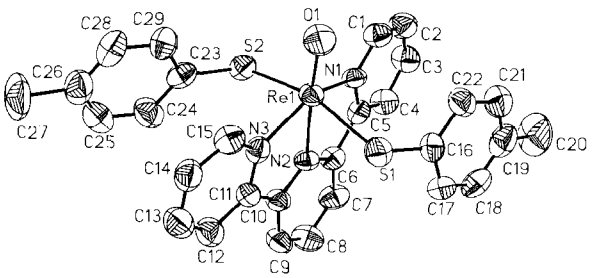

Fig. 3. A perspective view of [ReO(SC_6H_4Me-*p*)$_2$(terpy)]$^+$ illustrating the geometry and labeling of the cation. Ellipsoids represent 50% probability.

TABLE 9. Selected bond lengths (Å) and angles (°) in the cation [ReO(SC_6H_4Me-*p*)$_2$(terpy)]$^+$

Re1–S1	2.381(2)		
Re1–S2	2.381(2)		
Re1–O1	1.677(6)		
Re1–N1	2.085(6)		
Re1–N2	2.187(6)		
Re1–N3	2.101(6)		
S1–C16	1.785(8)		
S2–C23	1.768(8)		
Re1–S1–C16	106.2(3)	S2–Re1–N2	81.3(2)
Re1–S2–C23	109.1(3)	S2–Re1–N3	89.1(2)
S1–Re1–S2	160.39(7)	O1–Re1–N1	102.4(2)
S1–Re1–O1	99.7(2)	O1–Re1–N2	174.8(2)
S1–Re1–N1	94.3(2)	O1–Re1–N3	111.1(2)
S1–Re1–N2	79.3(2)	N1–Re1–N2	72.7(2)
S1–Re1–N3	82.3(2)	N1–Re1–N3	146.4(2)
S2–Re1–O1	99.9(2)	N2–Re1–N3	73.8(2)
S2–Re1–N1	83.1(2)		

The six ligands around rhenium form a distorted octahedron. The ligand donor atoms *cis* to the multiply bound oxo ligand are bent away from the oxygen atom: the angles are 102.4(2), 111.1(2), 99.7(2) and 99.9(2)° for N1, N3 and the two sulfur atoms, respectively. The rhenium–oxygen bond length is 1.677(6) Å, typical for rhenium(V) monooxo complexes (Table 10) and shorter than that usually assigned as a Re–O single bond (2.04 Å) [25] or a Re=O double bond (1.74–1.79 Å in the O=Re^v=O core) [26, 27]. This implies some triple bond character in the rhenium–oxygen bond in this complex.

The two aromatic thiolato ligands are equivalent. Both rhenium–sulfur bond lengths are 2.381(2) Å which is only slightly longer than most of the reported values for five-coordinate rhenium(V)–monooxo–thiolato complexes (2.31–2.38 Å, Table 10). Both [Re^{v}O(SC_6H_4Me-*p*)$_2$(terpy)]$^+$ and [Re^{v}O(SR)$_4$]$^-$ complexes contain the (Re^{v}O)$^{3+}$ core, so the difference in length is most likely steric, the six-coordinate complex lying at the high end of the range. Slightly shorter Re–S distances are observed in six-coordinate rhenium(III) complexes of the form [Re(SPh)$_2$(dip)$_2$]$^+$ (viz. 2.30 Å) [6, 7]. It has been previously noted [8, 28] that metal–thiolato bond lengths in six-coordinate rhenium(III) and technetium(III) complexes are nearly equivalent to those in five-coordinate complexes containing (Re^{v}O)$^{3+}$ and (Tc^{v}O)$^{3+}$ cores. Presumably the strong e^- donating ability of the oxo ligand compensates fairly well for the change in metal oxidation state making these M–S bond lengths com-

TABLE 10. Rhenium–oxygen and rhenium–sulfur bond lengths in selected rhenium(V)–oxo species

Compound	Re–O (Å)	Re–S (Å)	Reference
[ReO(SC_6H_4Me-*p*)$_2$(terpy)]$^+$	1.677(6)	2.381(2)	this work
[ReO(SPh)$_4$]$^-$	1.686(9)	2.340(3)	2
	1.66(1)	2.33(1)	30
[ReO($SC_6H_2Me_3$)$_4$]$^-$	1.65(1)	2.33(2)	3
[ReO($SC_6H_3Pr^i_2$)$_4$]$^-$	1.70(2)	2.35(2)	3
[ReO(SCH_2CH_2S)$_2$]$^-$	1.673(4)	2.31(1)	31
[ReO(SC_6H_4S)$_2$]$^-$	1.663(4)	2.315(3)	31
[ReO($SC_6H_4SiMe_3$-*o*)$_4$]$^-$	1.625(8)	2.38(1)	32
[ReO(SC(O)C(O)S)$_2$]$^-$	1.674(7)	2.332(6)	33

TABLE 11. Rhenium–oxygen and rhenium–nitrogen bond lengths in selected rhenium(V)–oxo species

Compound	Re–O (Å)	Re–N (Å)	Reference
$[ReO(SC_6H_4Me\text{-}p)_2(terpy)]^+$	1.677(6)	2.187(6), central 2.09(1), distal	this work
$[ReO_2py_4]^+$	1.76(1)	2.15(1)	27
$[ReO_2(en)_2]^+$	1.765(6)	2.16(2)	27
$[ReO_2(py\text{-}4\text{-}Me)_4]^+$	1.75(2)	2.14(2)	26
$[ReO(OEt)Cl_2py_2]$	1.684(7), oxo 1.896(6), OEt	2.138(8)	34
$[Re_2O_3py_4Cl_4]$	1.74(3), terminal 1.92(3), bridging	2.15(3)	35
$[ReO(bpy)Me(CH_2SiMe_3)_2]$	1.681(4)	2.127(5), *trans* to Me 2.359(5), *trans* to oxo	36

TABLE 12. Summary of geometries of terpy ligands in transition metal complexes[a]

N···N[b] (Å)	N···N···N (°)	N–M–N[c] (°), α	Twist angle[d] (°)	Bite[e] = 2 sin(α/2)	No. of entries[f]
Seven-coordinate metal environments					
2.564(2)	109.0(7)	71(1)	9(5)	1.16(2)	6
2.52–2.59	106–110	69–75	4.2–16.5	1.1–1.2	
Six-coordinate metal environments					
2.576(6)	105.5(4)	78.8(3)	4.3(4)	1.269(3)	48
2.47–2.76	100–113	75–84	0.4–13	1.22–1.32	
Five-coordinate metal environments					
2.56(1)	103.7(3)	78.9(5)	3.7(4)	1.275(5)	37
2.45–2.69	101–109	66–85	0.3–10.1	1.20–1.31	
Four-coordinate metal environments					
2.58(4)	101.9(4)	82(1)	4(2)	1.305(4)	8
2.43–2.86	101–104	73–92	1–17	1.29–1.32	
For comparison to the title structure: $[ReO(SC_6H_4Me\text{-}p)_2(terpy)]^+$					
2.56(3)	103.3(3)	73(1)	6(2)	1.19	

[a]This tabulation includes only those structures for which coordinates are recorded in the Cambridge Structural Database [24]. Omitted are bridging-μ structures. No eight-coordinate metal–terpy environments were found. The upper lines give the mean; lower lines the range. [b]N(outer)···N(middle) distance. [c]N(outer)–M–N(middle), also known as the bite angle. [d]Dihedral angle between the outer py ring and the middle py ring. [e]Ref. 29. [f]Some entries represent multiple occurrences of terpy within the same structure.

parable. In the absence of the multiply bound oxo ligand, technetium–thiolato bond lengths tend to increase with decreasing metal oxidation state [11] because the thiolato ligand functions primarily as a σ-donor, and it is predicted that rhenium would exhibit similar characteristics. The Re–S–C angles of 106.2(3) and 109.1(3)° in the title complex are approximately tetrahedral values.

The rhenium–nitrogen bond lengths are 2.187(6) and 2.093(11) Å for the central and distal positions, respectively. This complex comprises the first rhenium–terpy structure published, and Table 11 contains related rhenium(V)–bpy and rhenium(V)–py derivatives for structural comparison. Although the rhenium–nitrogen distances in the title structure are both longer ($Re–N_{central}$) and shorter ($Re–N_{distal}$) than the comparison values in Table 11, the average (2.12(5) Å) is well within the range of rhenium(V)–nitrogen lengths in related complexes.

There is a slight non-planarity in the tridentate terpy ligand due to the twist of the individual py rings. The dihedral angles between the outer and middle py rings are 4.1 and 7.1°. The rings of the terpy ligand in transition metal complexes are usually more coplanar than this, but larger deviations from coplanarity, as high as 17°, have also been observed [24]. The rhenium and oxygen atoms do not occupy the plane of the three nitrogen donor atoms, lying 0.07 and 0.17 Å from it, respectively. To describe the bond angles in metal–terpy complexes, the measure 'bite angle α' and 'bite' are often used. The bite angle is defined by the angle $N_{central}–Re–N_{distal}$, whereas the bite equals $2\sin(\alpha/2)$

[29]. For an ideal, undistorted, planar terpyridine ligand, α would be 60° corresponding to a bite of 1. In $[ReO(SC_6H_4Me\text{-}p)_2(terpy)]PF_6$ the bite angles are 72.2(2) and 73.8(2)° and the bite is 1.18 and 1.20. In most other metal–terpy complexes the bite and bite angle are higher. Table 12 contains a listing of terpy geometrical parameters in metal complexes, including bite and bite angle. On average, the N···N distances remain fairly constant throughout a variety of coordination numbers. The $N_{distal}\cdots N_{central}\cdots N_{distal}$ angle, however, reflects steric placement as it decreases with lower coordination number. The title structure $[ReO(SC_6H_4Me\text{-}p)_2(terpy)]^+$ is normal with regard to the range of N···N distances and the N···N···N angles in six-coordinate complexes. However its bite angle is unusual. Even though there is quite a bit of variance in bite angles in six-coordinate complexes, the average bite angle in $[ReO(SC_6H_4Me\text{-}p)_2(terpy)]^+$ is smaller than that in all other six-coordinate complexes; this parameter tends to decrease with increasing coordination number. The 'bite' parameter is also relatively smaller than that for other six-coordinate complexes; it, too, tends to decrease with increasing coordination number. Both of these parameters (bite and bite angle) indicate that in $[ReO(SC_6H_4Me\text{-}p)_2(terpy)]^+$ the terpy ligand is less deformed than in most other six-coordinate and lower coordinate complexes. Since in $[ReO(SC_6H_4Me\text{-}p)_2(terpy)]^+$, the terpy ligand shares the equatorial plane with the closely bound oxo ligand, steric pressure by the oxo atom may contract the ideal coordination sites for the three remaining equatorial sites, making them less than orthogonal.

Supplementary material

A complete set of crystallographic data for $[ReO(SC_6H_4Me\text{-}p)_2(terpy)]PF_6$ including experimental parameters, thermal parameters, hydrogen atomic coordinates, bond lengths and angles and structure factors is available from author M.J.H. upon request.

Acknowledgements

Financial support was provided by the National Institute of Health grants nos. HL-21276 and CA-42179 (E.D.). The diffractometer used herein was purchased through an NSF equipment grant to Wayne State University. The student exchange program for J. Rall was financially supported by the German Academic Exchange Service (DAAD).

References

1 J. R. Dilworth, B. D. Neaves, J. P. Hutchinson and J. A. Zubieta, *Inorg. Chim. Acta, 65* (1982) L223.
2 A. C. McDonell, T. W. Hambley, M. R. Snow and A. G. Wedd, *Aust. J. Chem., 36* (1983) 253.
3 P. J. Blower, J. R. Dilworth, J. P. Hutchinson, T. Nicholson and J. A. Zubieta, *Inorg. Chim. Acta, 90* (1984) L27.
4 P. J. Blower, J. R. Dilworth, J. P. Hutchinson and J. A. Zubieta, *J. Chem. Soc., Dalton Trans.,* (1985) 1533.
5 T. Nicholson, P. Lombardi and J. Zubieta, *Polyhedron, 6* (1987) 1577.
6 L. Chang, S.-I. Aizawa, M. J. Heeg and E. Deutsch, *Inorg. Chem., 30* (1991) 4920.
7 L. Chang, E. Deutsch and M. J. Heeg, *Transition Met. Chem.,* (1993) in press.
8 T. Konno, M. J. Heeg and E. Deutsch, *Inorg. Chem., 27* (1988) 4113.
9 T. Konno, J. R. Kirchhoff, W. R. Heineman and E. Deutsch, *Inorg. Chem., 28* (1989) 1174.
10 T. Konno, M. J. Heeg and E. Deutsch, *Inorg. Chem., 28* (1989) 1694.
11 T. Konno, R. Seeber, J. R. Kirchhoff, W. R. Heineman, E. Deutsch and M. J. Heeg, *Transition Met. Chem.,* (1993) in press.
12 T. Konno, M. J. Heeg, J. A. Stuckey, J. R. Kirchhoff, W. R. Heineman and E. Deutsch, *Inorg. Chem., 31* (1992) 1173.
13 T. Konno, J. R. Kirchhoff, W. R. Heineman, E. Deutsch and M. J. Heeg, *J. Chem. Soc., Dalton Trans.,* (1992) 3069.
14 B. E. Wilcox, D. M. Ho and E. Deutsch, *Inorg. Chem., 28* (1989) 1743.
15 B. E. Wilcox, D. M. Ho and E. Deutsch, *Inorg. Chem., 28* (1989) 3917.
16 E. Deutsch and K. Libson, *Comments Inorg. Chem., 3* (1984) 83; M. J. Clarke and L. Podbielski, *Coord. Chem. Rev., 78* (1987) 253; C. L. Jones, in G. Wilkinson, R. D. Gillard and J. McCleverty (eds.), *Comprehensive Coordination Chemistry,* Vol. 6, Pergamon, Oxford, 1987, p. 881; A. M. Verbruggen, *Eur. J. Nucl. Med., 17* (1990) 346.
17 N. P. Johnson, C. J. L. Lock and G. Wilkinson, *Inorg. Synth., 9* (1967) 145.
18 F. Weingart, J. Rall, D. M. Ho, M. J. Heeg, F. Tisato and E. Deutsch, manuscript in preparation.
19 *Sadtler Standard Infrared Spectra,* Vol. 16, Sadtler Research Laboratories, Philadelphia, No. 15807-15809.
20 G. Rouchias, *Chem. Rev., 74* (1974) 543.
21 F. A. Cotton and F. J. Lippard, *Inorg. Chem., 5* (1966) 9; M. Freni, D. Giusto, P. Romiti and G. Minghetti, *Gazz. Chim. Ital., 99* (1969) 286.
22 T. Lis, *Acta Crystallogr., Sect. B, 32* (1976) 2707; *33* (1977) 944; S. R. Fletcher and A. C. Skapski, *J. Chem. Soc., Dalton Trans.,* (1972) 1073; R. Battistuzzi, T. Manfredini, L. P. Battaglia, A. B. Corradi and A. Marzotto, *J. Cryst. Spectrosc., 19* (1989) 513; G. Ciani, G. D'Alfonso, P. Romiti, A. Sironi and M. Freni, *Inorg. Chim. Acta, 72* (1983) 29.
23 G. Bandoli, U. Mazzi, E. Roncari and E. Deutsch, *Coord. Chem. Rev., 44* (1982) 191; F. A. Cotton and G. Wilkinson, *Advanced Inorganic Chemistry,* Wiley, New York, 4th edn., 1980, p. 153.
24 F. H. Allen, O. Kennard and R. Taylor, *Acc. Chem. Res., 16* (1983) 146.
25 F. A. Cotton and F. J. Lippard, *Inorg. Chem., 5* (1966) 416, and refs. therein.
26 J. W. Johnson, J. F. Brody, G. B. Ansell and S. Zentz, *Inorg. Chem., 23* (1984) 2415.

27 C. J. L. Lock and G. Turner, *Acta Crystallogr., Sect. B, 34* (1978) 923.
28 B. Chen, M. J. Heeg and E. Deutsch, *Inorg. Chem., 31* (1992) 4683, and refs. therein.
29 B. N. Figgis, E. S. Kucharski and A. H. White, *Aust. J. Chem., 36* (1983) 1563.
30 T. Nicholson, P. Lombardi and J. Zubieta, *Polyhedron, 6* (1987) 1577.
31 W. Clegg, S. Boyde and C. D. Garner, *Acta Crystallogr., Sect. C, 44* (1988) 172.
32 E. Block, H. Kang, G. Ofori-Okai and J. Zubieta, *Inorg. Chim. Acta, 156* (1989) 27.
33 R. Mattes and H. Weber, *Z. Anorg. Allg. Chem., 474* (1981) 216.
34 C. J. L. Lock and G. Turner, *Can. J. Chem., 55* (1977) 333.
35 C. J. L. Lock and G. Turner, *Can. J. Chem., 56* (1978) 179.
36 W. A. Herrmann, J. G. Kuchler, G. Weichselbaumer, E. Herdtweck and P. Kiprof, *J. Organomet. Chem., 372* (1989) 351.